

LESSONS FROM THE SHORT GRB 170817A – THE FIRST GRAVITATIONAL WAVE DETECTION OF A BINARY NEUTRON STAR MERGER

JONATHAN GRANOT¹, DAFNE GUETTA², AND RAMANDEEP GILL^{1,3}*Draft version December 14, 2024*

ABSTRACT

The first, long awaited, detection of a gravitational wave (GW) signal from the merger of a binary neutron-star (NS-NS) system was finally achieved, and was also accompanied by an electromagnetic counterpart – the short-duration GRB 170817A. It occurred in the nearby ($D \approx 40$ Mpc) elliptical galaxy NGC 4993, and showed optical, IR and UV emission from half a day up to weeks after the event, as well as late time X-ray (at ≥ 9 days) and radio (at ≥ 17 days) emission. There was a delay of $\Delta t \approx 1.74$ s between the GW merger chirp signal and the prompt-GRB emission onset, and an upper limit of $\theta_{\text{obs}} < 28^\circ$ was set on the viewing angle w.r.t the jet's symmetry axis from the GW signal. In this letter we examine some of the implications of these groundbreaking observations. The delay Δt sets an upper limit on the prompt-GRB emission radius, $R_\gamma \lesssim 2c\Delta t/(\theta_{\text{obs}} - \theta_0)^2$, for a jet with sharp edges at an angle $\theta_0 < \theta_{\text{obs}}$. GRB 170817A's relatively low isotropic equivalent γ -ray energy-output and peak νF_ν photon energy suggest either a viewing angle slightly outside the jet's sharp edge, $\theta_{\text{obs}} - \theta_0 \sim (0.05 - 0.1)(100/\Gamma)$, or that the jet does not have sharp edges and the prompt emission was dominated by less energetic material along our line of sight, at $\theta_{\text{obs}} \gtrsim 2\theta_0$. Finally, we consider the type of remnant that is produced by the NS-NS merger and find that a relatively long-lived (> 2 s) massive NS is strongly disfavored, while a hyper-massive NS of lifetime ~ 1 s appears to be somewhat favored over the direct formation of a black hole.

Subject headings: gamma rays: bursts — stars: neutron — gravitational waves

1. INTRODUCTION

The first discovery of gravitational waves (GWs) from two coalescing black holes (BHs) by the Advanced Laser Interferometer Gravitational-wave Observatory (LIGO) ushered in a new era of GW astronomy (Abbott et al. 2016a). It was soon followed by two other BH-BH mergers that firmly established LIGO's sensitivity to robustly detect such sources out to $\sim \text{Gpc}$ distances. LIGO can also detect GWs from compact binary mergers involving neutron stars (NSs), NS-NS and NS-BH, at a volume-weighted mean distance of ~ 70 Mpc and ~ 110 Mpc, respectively, and set an upper limit of $12,600 \text{ Gpc}^{-3} \text{ yr}^{-1}$ on the NS-NS merger rate (90% CL; Abbott et al. 2016b).

An electromagnetic (EM) counterpart to the GW signal from a BH-BH merger is not expected (in most scenarios). However, its detection is of great importance in NS-NS or NS-BH mergers, which have been posited to be the progenitors of short-hard gamma-ray bursts (SGRBs; e.g. Eichler et al. 1989; Narayan et al. 1992). A NS-NS merger leads to the formation of a BH, possibly preceded by a short-lived hypermassive NS. Accretion onto the BH launches a relativistic jet reaching bulk Lorentz factors $\Gamma \gtrsim 100$ and powering a SGRB – a short ($\lesssim 2$ s) intense flash of γ -rays with a typical (νF_ν -peak) photon energy $E_{\text{pk}} \sim 400$ keV and total isotropic-equivalent energy release $E_{\gamma, \text{iso}} \simeq 10^{49} - 10^{51}$ erg (Nakar 2007; Berger 2014). On the other hand, long-soft GRBs are known to originate from the death of massive stars, via their associa-

tion with star-forming regions and type Ic core-collapse supernovae (e.g., Woosley & Bloom 2006).

The unprecedented observation of an SGRB (von Kienlin et al. 2017) coincident with the detection of GWs from coalescing binary NSs (CITE) in an elliptical galaxy presents the long-awaited "smoking gun" that binary NS mergers give rise to SGRBs. Rapid follow-up observations by detectors across the EM spectrum both increase the positional accuracy of the source in the host galaxy and yield critical information regarding jet geometry, merger ejecta, and r-process elements (e.g. Rosswog, Piran, & Nakar 2013).

In §2 the delay between the GW and SGRB signals is used to constrain the location of the γ -ray emission region. In §3 the prompt γ -ray emission properties are used to constrain the GRB jet's angular structure and our viewing angle θ_{obs} from the jet's symmetry axis. The constraints on the type of remnant produced by the NS-NS merger are discussed in §4. Finally, the implications of this work are discussed in §5.

2. THE TIME DELAY BETWEEN THE GW SIGNAL AND SGRB: AN UPPER LIMIT ON THE EMISSION RADIUS

A delay of $\Delta t = 1.74 \pm 0.05$ s was found between the binary merger GW chirp signal and GRB 170817A's γ -ray emission onset (Abbott et al. 2017a). Such a delay can arise from one or more causes, and may provide important information on the merging system and the merger process. Moreover, the GW signal and known distance to the host galaxy set an upper limit on the viewing angle of $\theta_{\text{obs}} < 28^\circ \approx 0.49$ rad (Abbott et al. 2017b).

One possible cause for such a delay is the formation of a short lived, $t_{\text{HMNS}} \lesssim 1$ s, hypermassive NS, whose collapse forms a BH surrounded by an accretion disk that launch a relativistic jet. In order to produce a GRB, the

¹ Department of Natural Sciences, The Open University of Israel, 1 University Road, POB 808, Raanana 4353701, Israel

² Department of Physics and Optical Engineering, ORT Braude College, Karmiel 21982, Israel

³ Physics Department, Ben-Gurion University, P.O.B. 653, Beer-Sheva 84105, Israel

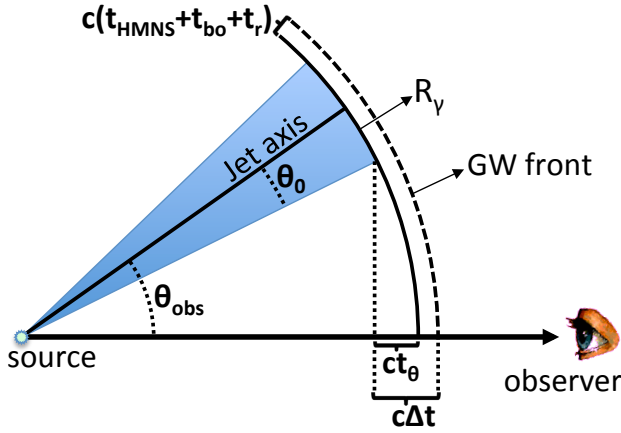


FIG. 1.— Illustration of the γ -ray to GW geometrical time delay t_θ for a jet viewed from outside of its aperture.

jet must first bore its way through the dynamical ejecta and/or neutrino driven wind that was launched during t_{HMNS} , causing a time delay of t_{bo} , which may typically be a good fraction of a second (e.g., Moharana & Piran 2017; Nakar & Piran 2017). Once the jet breaks out of this wind or outflow, it quickly accelerates to ultra-relativistic speeds, where compactness arguments suggest that its Lorentz factor during the prompt γ -ray emission, at a distance of R_γ from the central source, is $\Gamma \gtrsim 100$. The delay t_r in the γ -ray emission onset for an on-axis observer that is caused by this acceleration phase and a possible coasting phase until the jet reaches R_γ , due to the jet's motion along the radial direction at speeds slightly less than c , is typically negligible (usually $t_r \lesssim R_\gamma/2c\Gamma^2 = 1.7R_{\gamma,13}/\Gamma_{2.5}^2$ ms).

When the outflow in the jet reaches the γ -ray emission radius, R_γ , it radiates the prompt GRB. For a jet viewed off-axis from $\theta_{\text{obs}} > \theta_0$ this angular offset causes a geometrical delay because of the additional path length of the radiation from the edge of the jet closest to the observer compared to an on-axis observer (see Fig. 1),

$$t_\theta = \frac{R_\gamma}{c} [1 - \cos(\Delta\theta)] \approx \frac{R_\gamma}{2c} \Delta\theta^2 = 1.67R_{\gamma,13}\Delta\theta_{-1}^2 \text{ s}, \quad (1)$$

where $\Delta\theta \equiv \theta_{\text{obs}} - \theta_0 = 0.1\Delta\theta_{-1}$. Altogether, the total delay is the sum of all the different causes, $\Delta t \geq t_{\text{HMNS}} + t_{\text{bo}} + t_r + t_\theta > t_\theta$. Therefore, one can use the fact that $\Delta t > t_\theta \approx R_\gamma\Delta\theta^2/2c$ to set an upper limit on R_γ ,

$$R_\gamma < \frac{c\Delta t}{1 - \cos(\Delta\theta)} \approx \frac{2c\Delta t}{\Delta\theta^2} = 6 \times 10^{12} \left(\frac{\Delta t}{1 \text{ s}} \right) \Delta\theta_{-1}^{-2} \text{ cm}. \quad (2)$$

This upper limit $R_{\gamma,\text{max}}$ on R_γ is plotted in Fig. 2 for $(\Delta t, \theta_0) = (2 \text{ s}, 0), (1 \text{ s}, 0), (2 \text{ s}, 0.1), (2 \text{ s}, 0.3)$. The afterglow lightcurve fits suggest $\Delta\theta \gtrsim 0.2$ (Granot et al. 2017), as illustrated by the vertical lines in Fig. 2. Together with the measured Δt this implies $R_\gamma \lesssim 1.7 \times 10^{12}(\Delta\theta/0.25)^{-2}$ cm. Such a limit is very restrictive for models of the GRB prompt emission and outflow acceleration. Note that any estimate or lower limit on the other time delays besides t_θ that contributing to Δt could make this upper limit on R_γ even stricter. A long-lived HMNS, $t_{\text{HMNS}} \gtrsim 0.3 - 1$ s for which one might expect $t_{\text{bo}} \gtrsim 0.5$ s would imply a lower $t_\theta \lesssim 0.5 - 1$ s (see the thin red line in Fig. 2 for $t_\theta = 0.5$ s as an illustration of such a case).

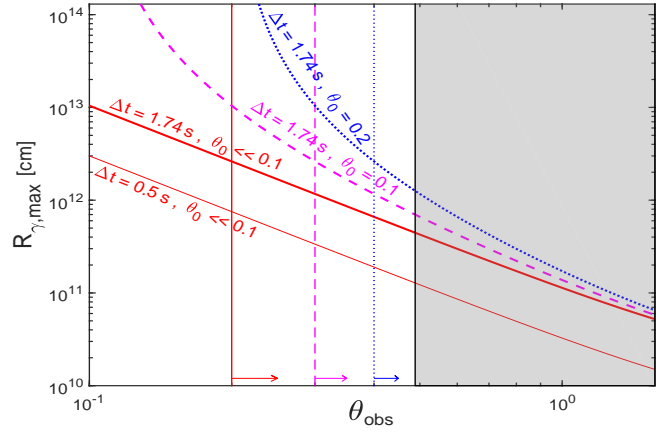


FIG. 2.— The upper limit $R_{\gamma,\text{max}}$ on the γ -ray emission radius from the geometrical time delay, t_θ , as a function of the viewing angle, θ_{obs} , for four sets of $(\Delta t, \theta_0)$ values. The corresponding vertical lines are tentative lower limits on θ_{obs} from the fact that afterglow fits suggest $\Delta\theta \gtrsim 0.2$. The gray region is excluded by the GW signal.

3. CONSTRAINING THE VIEWING ANGLE FROM THE PROMPT GRB EMISSION

Since the prompt GRB emission was observed, we are either (i) within the jet's initial aperture ($\theta_{\text{obs}} < \theta_0$) or beaming cone ($\theta_{\text{obs}} < \theta_0 + 1/\Gamma$), (ii) slightly outside of a sharp edged jet, $\theta_{\text{obs}} > \theta_0$ but $\Gamma\Delta\theta$ is not too large for the prompt emission to be detectable, or (iii) well outside the core of a jet ($\theta_{\text{obs}} \gtrsim 2\theta_0$) that (more realistically) does not have very sharp edges and the prompt GRB is produced by relativistic outflow along our line of sight. An alternative that is not discussed here in detail is that the prompt GRB and possibly the afterglow arise from the breakout of a mildly relativistic cocoon (Kasliwal et al. 2017; Evans et al. 2017; Troja, et al. 2017; Abbott et al. 2017a).

In case (i) a bright and usually highly variable prompt γ -ray emission is expected, with relatively high values of the isotropic equivalent γ -ray energy output, $E_{\gamma,\text{iso}}$, and peak photon energy, E_p . GRB 170817A had a fluence of $f = (2.8 \pm 0.2) \times 10^{-7}$ erg cm $^{-2}$ (10–1000 keV) corresponding to $E_{\gamma,\text{iso}} = (5.36 \pm 0.38) \times 10^{46} D_{40\text{Mpc}}^2$ erg and $E_p = 82 \pm 21$ keV (von Kienlin et al. 2017). The initial half-second spike had $E_p = 185 \pm 62$ keV while the softer tail had $E_p = 40 \pm 6$ keV and a black-body spectrum (Abbott et al. 2017c). For SGRBs with known redshifts typically $E_{\gamma,\text{iso}} \sim 10^{49} - 10^{51}$ erg, i.e. $\sim 3 - 4$ decades above GRB 170817A, and an intrinsic $\langle(1+z)E_p\rangle \sim 500 - 600$ keV, several times larger than in GRB 170817A. The low $E_{\gamma,\text{iso}}$ and E_p in GRB 170817A suggest a line of sight is outside of the jet, $\theta_{\text{obs}} > \theta_0$, arguing against case (i) above ($\theta_{\text{obs}} > \theta_0$ also correspond to most of the total solid angle for narrow jets and are thus more likely for events associated with a binary merger GW signal), as do the afterglow observations.

In case (ii) the observed low $E_{\gamma,\text{iso}}$ and E_{peak} values are caused by a viewing angle outside of the jet's initial aperture, $\theta_{\text{obs}} > \theta_0$. For a uniform jet with sharp edges the ratio of off-axis to on-axis E_p and $E_{\gamma,\text{iso}}$ are (Granot

et al. 2002, 2005; Granot & Ramirez-Ruiz 2012):

$$\frac{E_p(\theta_{\text{obs}})}{E_p(0)} \equiv a \approx \begin{cases} 1 & \theta_{\text{obs}} < \theta_0 \\ \frac{1}{1+(\Gamma\Delta\theta)^2} \sim (\Gamma\Delta\theta)^{-2} & \theta_{\text{obs}} > \theta_0 \end{cases}, \quad (3)$$

$$\frac{E_{\gamma,\text{iso}}(\theta_{\text{obs}})}{E_{\gamma,\text{iso}}(0)} \approx \begin{cases} 1 & \theta_{\text{obs}} < \theta_0 \\ a^2 \sim (\Gamma\Delta\theta)^{-4} & 1 < \frac{\theta_{\text{obs}}}{\theta_0} < 2 \\ \frac{(\Gamma\theta_0)^2}{(\Gamma\Delta\theta)^6} \sim \frac{(\Gamma\theta_0)^2}{(\Gamma\theta_{\text{obs}})^6} & \theta_{\text{obs}} > 2\theta_0 \end{cases}, \quad (4)$$

where we assume that $\Gamma\theta_0 \gg 1$, as is inferred for GRBs. For $1 < \theta_{\text{obs}}/\theta_0 < 2$, $E_{\gamma,\text{iso}}(\theta_{\text{obs}})/E_{\gamma,\text{iso}}(0) \sim (\Gamma\Delta\theta)^{-4}$ already reaches its inferred value of $\sim 10^{-4} - 10^{-3}$ for $\Delta\theta \sim (0.05 - 0.1)(100/\Gamma) \lesssim 0.05 - 0.1$, where $\Gamma \gtrsim 100$ for GRBs. I.e. in case (ii) we are only slightly the jet's outer edge. For GRB 170817A this implies $E_p(\theta_{\text{obs}})/E_p(0) = a = [E_{\gamma,\text{iso}}(\theta_{\text{obs}})/E_{\gamma,\text{iso}}(0)]^{1/2} \sim 30 - 100$ and hence $E_p(0) \sim 3 - 8$ MeV (or $\sim 5 - 20$ MeV for the main half-second initial spike), which is unusually high for a SGRB of typical $E_{\gamma,\text{iso}}$. This favors case (iii), as do

Case (iii) allows large off-axis viewing angles $\theta_{\text{obs}} \gtrsim 2\theta_0$ for which the afterglow emission from the jet's core peaks and joins the post jet-break on-axis lightcurve at $t_{\text{peak}} \propto \theta_{\text{obs}}^2$ (e.g. Granot et al. 2002; Nakar, Piran & Granot 2002). Moreover, in this case we expect in addition to this off-axis emission from the jet's core also a contribution to the afterglow lightcurve from the material along the line of sight after it produces the prompt GRB. The latter may dominate at early times before $t_{\text{peak}}(\theta_{\text{obs}})$ while the emission from the jet's energetic core ($\theta < \theta_0$) is still strongly beamed away from the observer. At $t \gtrsim t_{\text{peak}}$ the line of sight enters the beaming cone of the jet's core so that its larger energy causes its emission to dominate over that from the less energetic material along the line of sight at $t \gtrsim t_{\text{peak}}$. Therefore, in case (iii) a shallower rise to the peak flux at t_{peak} may be expected (e.g., Granot et al. 2002; Eichler & Granot 2006; Granot & Kumar 2003).

The early afterglow emission from material along our line of sight in case (iii) may be estimated by assuming spherical emission with the local isotropic equivalent kinetic energy $E_{k,\text{iso}} \sim E_{\gamma,\text{iso}} \approx 4.4 \times 10^{46} D_{40\text{Mpc}}^2$ erg. The latter assumption is reasonable at sufficiently early times when one expects that $E_{k,\text{iso}}$ has not greatly changed from its initial value. The flux densities in the relevant power-law segments of the spectrum are (Granot & Sari 2002, after the local deceleration time):

$$F_{\nu > \nu_c, \nu_m} = 1.18 \epsilon_{e,-1}^{p-1} \epsilon_{B,-2}^{\frac{p-2}{4}} t_{\text{days}}^{(2-3p)/4} \nu_{14.7}^{-p/2} \mu\text{Jy}, \quad (5)$$

$$F_{\nu_m < \nu < \nu_c} = 0.0131 \epsilon_{e,-1}^{p-1} \epsilon_{B,-2}^{\frac{p+1}{4}} n_0^{1/2} t_{\text{days}}^{\frac{3-3p}{4}} \nu_{14.7}^{\frac{1-p}{2}} \mu\text{Jy}, \quad (6)$$

$$F_{\nu_a < \nu < \nu_m < \nu_c} = 196 \epsilon_{e,-1}^{-\frac{2}{3}} \epsilon_{B,-2}^{1/3} n_0^{\frac{1}{3}} t_{\text{days}}^{1/2} \nu_{9.93}^{1/3} \mu\text{Jy}, \quad (7)$$

with the numerical coefficient evaluated for $p = 2.2$. These fiducial values correspond to $\nu F_\nu \approx 10^{-15}$ erg cm $^{-2}$ s $^{-1}$ at $h\nu = 1$ keV for $\nu > \nu_c$, ν_m after one day, which is consistent with the Chandra upper limit (Margutti et al. 2017) of $F_X < 1.4 \times 10^{-15}$ erg cm $^{-2}$ s $^{-1}$ (0.3 – 10 keV) at 2.3 days. The corresponding optical magnitude for $\nu_m < \nu < \nu_c$ after one day is $\sim 28 - 29$, which would be extremely hard to detect. The radio upper limit of $F_{10\text{GHz}} < 15.4 \mu\text{Jy}$ at 1.39 days (Hallinan et al. 2017) is the quite constraining here, and favors low values of n_0 and/or ϵ_B . Therefore, even if such material

along the line of sight produce the observed GRB prompt mission, its afterglow emission would be very challenging to detect.

4. THE REMNANT OF THE NS-NS MERGER

The type of remnant that was produced during this NS-NS merger is rather uncertain. The chirp-mass was determined from the GW signal to be $\mathcal{M} \equiv (M_1 M_2)^{3/5} (M_1 + M_2)^{-1/5} = 1.188^{+0.004}_{-0.002} M_\odot$ (Abbott et al. 2017b) where M_1 and M_2 are the pre-merger (gravitational) masses of the two NSs. Figure 3 shows M_1 and M_2 as a function of their mass ratio, $q \equiv M_1/M_2 \leq 1$, along with the initial, pre-merger total mass if the system, $M_i = M_1 + M_2$. This measured chirp mass \mathcal{M} implies $M_i \geq 2.73 M_\odot$. The final mass of the remnant that left after the merger, M_f , can however be smaller (by about $\approx 7\%$; Timmes et al. 1996) because of before accounting for mass ejection and energy losses to gravitational waves and neutrinos during or shortly after the merger. Therefore, Fig. 3 also shows an estimate of the resulting final mass M_f after such a reduction (*dashed magenta line*) by assuming that $0.01 M_\odot$ of baryonic mass were ejected during the merger and using the relation between the baryonic (M_b) and gravitational (M_g) masses from Timmes et al. (1996), $M_b = M_g + 0.075 M_g^2$ in solar masses. The exact range of final masses that corresponds to each one of the outcomes (stable NS, supra-massive NS, HMNS, and BH) is uncertain and depends on the EOS. Nonetheless, it is evident that a stable NS remnant in GRB 170817A would require both approximately equal masses of the merging NSs, as well as a very stiff EOS. The immediate formation of a BH has been ruled out by the GW signal for GRB 170817A. Therefore, the mostly likely outcome is either a SMNS or a HMNS, but it is hard to distinguish between them.

For a long-lived (> 2 s) massive NS remnant, which includes a stable NS, a SMNS or a particularly long-lived HMNS, it is not clear what powers the SGRB GRB 170817A. A magnetar wind has a typical duration of the spindown time, which is typically much larger than the ≤ 2 s duration of GRB 170817A. Moreover, a near break-up initial spin period of $\lesssim 1$ ms is expected, resulting in a very large initial rotational energy, $E_{\text{rot}} \sim 10^{52.5} - 10^{53}$ erg, and in a relatively short initial spindown time, which does not exceed several years even for a typical pulsar-like surface magnetic dipole field strength (of $\sim 10^{12}$ G). Therefore, by the time of the the radio to X-ray observations within the first month after the event, at least a few percent of E_{rot} , i.e. $\gtrsim 10^{51}$ erg (and possibly most of E_{rot}) is extracted in the form of a roughly isotropic pulsar-type ultra-relativistic MHD wind. Such an energy in a relativistic wind is expected to produce a very bright afterglow emission as it interacts with the external medium, especially at a nearby distance of ≈ 40 Mpc, which is inconsistent with the multi-wavelength follow-up observations of GRB 170817A. Therefore, argueably, the most likely option is the formation of an HMNS with a lifetime $t_{\text{HMNS}} < \Delta t \approx 1.74$ s so that its collapse to a BH and subsequent accretion onto this BH could launch the jet that powered GRB 170817A, and still be consistent with the GRB's delayed onset w.r.t the GW chip signal.

5. DISCUSSION

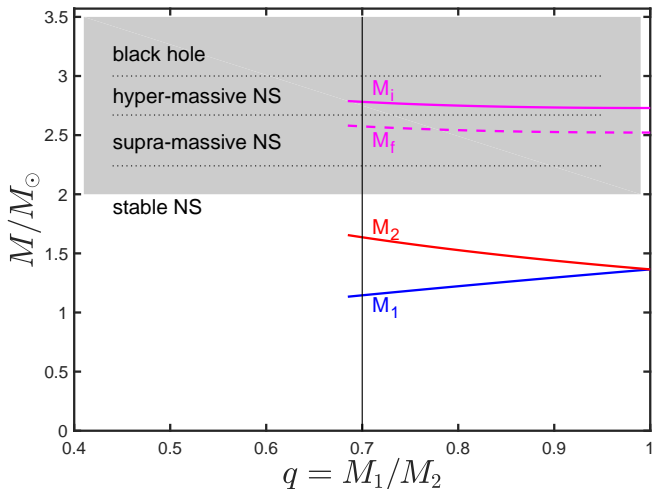


FIG. 3.— The possible pre-merger masses of the two NSs, M_1 (in blue) and M_2 (in red), as a function of their mass ratio $q \equiv M_1/M_2 \leq 1$, given the measured chirp mass, $\mathcal{M} \equiv (M_1 M_2)^{3/5} (M_1 + M_2)^{-1/5} = 1.188^{+0.004}_{-0.002} M_\odot$. Also shown is the system’s pre-merger total (gravitational) mass, M_{tot} , before (solid magenta line) and after (dashed magenta line) accounting for losses due to mass ejection, gravity waves and neutrinos during the merger (as described in the text). The vertical thin dashed line indicates the lower limit on q from the GW signal. Also shown schematically are the possible outcomes, in order of increasing final mass range: a stable NS, a SMNS, a HMNS, and a BH. The shaded region above $2M_\odot$ indicates the uncertainty in the mass limits dividing the different types of remnants.

We have addressed some implications of GRB 170817A observations, combining its EM emission, and the associated GW signal of the binary NS merger that triggered it – the first of its kind. In §2 we have used the observed time delay of $\Delta t = 1.74 \pm 0.05$ s between the GW chirp signal and the GRB onset in order to set an upper limit on the prompt GRB emission radius $R_\gamma \leq R_{\gamma, \text{max}} \approx 2c\Delta t/\Delta\theta^2$ for a uniform jet with sharp edges viewed from outside of its aperture (see Eq. (2) and Figs. 1, 2).

Next, in §3 we interpreted the relatively low measured values of $E_{\gamma, \text{iso}}$ and E_p for GRB 170817A in the context of a narrow GRB jet viewed off-axis, from outside of its initial aperture. For a uniform sharp-edged jet this suggests that our line of sight is only slightly outside of the jet $\Delta\theta \sim (0.05 - 0.1)(\Gamma/100)^{-1}$, which would in turn imply an unusually high on-axis $E_p(0) \sim 3 - 8$ MeV (or $\sim 5 - 20$ MeV for the main spike), and a relatively high $R_{\gamma, \text{max}}$. The implied high $E_p(0)$ and the expected afterglow lightcurves both favor an alternative picture (case (iii)), in which our viewing angle is larger ($\theta_{\text{obs}} \gtrsim 2\theta_0$) and the prompt emission arises from material along our line of sight that is less energetic than the jet’s core.

This picture implies a higher afterglow flux at very early times, keeps GRB 170817A well above the Amati relation ($E_p - E_{\gamma, \text{iso}}$ correlation) like most SGRBs, and induces no angular time delay t_θ . Since the radial time delay t_r is typically negligible for a highly-relativistic outflow, the observed delay $\Delta t \approx 1.74$ s would then likely be dominated by $t_{\text{HMNS}} \gtrsim 1$ s and $t_{\text{bo}} \sim 0.5$ s.

The latter conclusion is consistent with the arguments raised in §4 against a long-lived massive NS remnant (stable NS or SMNS). While a direct formation of a black hole might still be possible, given the systems expected final mass this would not be the case for many of the leading models for the NS equation of state (e.g. Abbott et al. 2017a). Moreover, it would require another origin for the delay time Δt , such as the radial time delay t_r for a mildly relativistic outflow. However, if the BH and GRB jet form immediately following the NS-NS merger, then there would be very little neutrino-driven wind in front of the jet’s head that would cause a significant fraction of its energy to be channeled into a cocoon, whose breakout might account for such a mildly relativistic outflow along our line of sight. These arguments appear to favor the formation of a short-lived HMNS, with a lifetime of $t_{\text{HMNS}} \sim 1$ s or so.

The first detection of a GW signal from the merger of a NS-NS system was observed in coincidence with GRB 170817A. We were apparently lucky in the sense that most NS-NS merger GW signals are expected without an associated GRB, since GRB jets are thought to be narrowly collimated, covering only a small fraction, $f_b \sim 10^{-2} - 10^{-1}$, of the total solid angle. On the other hand, the evidence for narrow jets in short-hard GRBs is much weaker than in long-soft GRBs, so it might be that the beaming factor f_b is larger than expected, which would require us to be somewhat less lucky to have observed the association with GRB 170817A. Moreover, it may very well be that our viewing angle θ_{obs} is not particularly small (since most of the solid angle is at large angles), but the jet does not have sharp edges as is often assumed mainly out of convenience, but instead has wide wings that extend out to large angles from its symmetry axis. In this case the prompt GRB emission in GRB 170817A was from such material with a low $E_{k, \text{iso}} \sim E_{\gamma, \text{iso}}$. A determination of θ_{obs} from the GW signal together with elaborate multi-wavelength afterglow observations could help determine the GRB jet angular structure, as well as constrain the prompt GRB emission radius R_γ .

JG and RG are supported by the Israeli Science Foundation under Grant No. 719/14. RG is supported by an Open University of Israel Research Fellowship.

REFERENCES

- Abbott, B. P., et al. 2016a, Phys. Rev. Lett., 116, 061102
 Abbott, B. P., et al. 2016b, ApJ, 832, 21
 Abbott, B. P., et al. 2017a, ApJ, 848, L13
 Abbott, B. P., et al. 2017b, Phys. Rev. Lett., 119, 161101
 Abbott, B. P., et al. 2017c, ApJ, 848, L12
 Barnes, K. and Kasen, D., 2013, ApJ775, 18B
 Berger, E. 2014, ARA&A, 52, 43
 Church, R. P., Levan, A. J., Davies, M. B., & Tanvir, N. 2011, MNRAS, 413, 2004
 Eichler, D., & Granot, J. 2006, ApJ, 641, L5
 Eichler, D., Livio, M., Piran, T., & Schramm, D. N. 1989, Nature, 340, 126
 Evans, P. A., et al. 2017, Science, 10.1126/science.aap9580
 Granot, J., et al. 2017, submitted to MNRAS (arXiv:1707.09433)
 Granot, J., & Kumar, P., 2003, ApJ, 591, 108
 Granot, J., Panaitescu, A., Kumar, P., & Woosley, S. E. 2002, ApJ, 570, L61
 Granot, J. & Sari, R. 2002, ApJ, 568, 820.
 Granot, J., Ramirez-Ruiz, E., & Perna, R. 2005, ApJ, 630, 1003

- Granot J., Ramirez-Ruiz E., 2012, in *Gamma-Ray Bursts*, eds. C. Kouveliotou, S. E. Woosley, & R. A. M. J. Wijers (CUP), chapter 11 (arXiv:1012.5101)
- Hallinan, G., et al. 2017, *Science*, doi:10.1126/science.aap9855
- Kasen, D. Fernandez, R. & Metzger, B.D. 2015, *MNRAS* 450, 1777
- Kasliwal, M. M., et al. 2017, *Science*, 10.1126/science.aap9455
- Margutti, R., et al. 2017, *ApJ*, 848, L20
- Metzger, B. D. 2017, *Living Rev. Rel.*, 20, 3 (arXiv:1610.09381)
- Moharana, R., & Piran, T. 2017, preprint, arXiv:1705.02598
- Nakar, E. 2007, *Phys. Rep.*, 442, 166
- Nakar, E., & Piran, T. 2017, *ApJ*, 834, 28
- Nakar, E., Piran, T., & Granot, J. 2002, *ApJ*, 579, 699
- Narayan, R., Paczynski, B., & Piran, T. 1992, *ApJ*, 395, L83
- Rosswog, S., Piran, T., & Nakar, E. 2013, *MNRAS*, 430, 2585
- Sari, R., Piran, T., & Narayan, R. 1998, *ApJ*, 497, L17.
- Smartt, S. J., et al. 2017, *Nature*, doi:10.1038/nature24303
- Timmes, F. X., Woosley, S. E., & Weaver, Thomas A. 1996, *ApJ*, 457, 834
- Troja, E., et al. 2017, *Nature*, doi:10.1038/nature24290
- von Kienlin, A., Meegan, C., & Goldstein, A. 2017, *GCN*, 21520, 1
- Woosley, S. E., & Bloom, J. S. 2006, *ARA&A*, 44, 507